HAL
open science

Regulation of Na+/H+ exchanger 1 allosteric balance by its localization in cholesterol- and caveolin-rich membrane microdomains.

Xavier Tekpli, Laurence Huc, Jérôme Lacroix, Mary Rissel, Mallorie Poët, Josette Noël, Marie-Thérèse Dimanche-Boitrel, Laurent Counillon, Dominique Lagadic-Gossmann

To cite this version:

Xavier Tekpli, Laurence Huc, Jérôme Lacroix, Mary Rissel, Mallorie Poët, et al.. Regulation of Na+/H+ exchanger 1 allosteric balance by its localization in cholesterol- and caveolin-rich membrane microdomains.. Journal of Cellular Physiology, 2008, 216 (1), pp.207-20. 10.1002/jcp.21395 . hal-00696172

HAL Id: hal-00696172

https://hal.science/hal-00696172v1

Submitted on 29 May 2020

HAL is a multi-disciplinary open access archive for the deposit and dissemination of scientific research documents, whether they are published or not. The documents may come from teaching and research institutions in France or abroad, or from public or private research centers.

L'archive ouverte pluridisciplinaire **HAL**, est destinée au dépôt et à la diffusion de documents scientifiques de niveau recherche, publiés ou non, émanant des établissements d'enseignement et de recherche français ou étrangers, des laboratoires publics ou privés.

Journal of Cellular Physiology

Regulation of Na^+/H^+ Exchanger 1 Allosteric Balance by Its Localization in Cholesterol- and Caveolin-Rich Membrane Microdomains

XAVIER TEKPLI,[1,2] LAURENCE HUC,[1,2] JÉRÔME LACROIX,[3] MARY RISSEL,[1,2] MALLORIE POËT,[3] JOSETTE NOËL,[4] MARIE-THÉRÈSE DIMANCHE-BOITREL,[1,2] LAURENT COUNILLON,[3] AND DOMINIQUE LAGADIC-GOSSMANN[1,2]*

[1]*INSERM U620, Equipe Labellisée Ligue contre Le Cancer, Rennes Cedex, France*

[2]*Université Rennes 1, IFR 140, Rennes Cedex, France*

[3]*CNRS UMR6548, Faculté des Sciences Parc Valrose, Université Nice-Sophia Antipolis, Nice Cedex 2, France*

[4]*Département de Physiologie, Université de Montréal, Montréal, Quebec, Canada*

The Na^+/H^+ exchanger 1, which plays an essential role in intracellular pH regulation in most tissues, is also known to be a key actor in both proliferative and apoptotic processes. Its activation by H^+ is best described by the Monod–Wyman–Changeux model: the dimeric NHE-1 oscillates between a low and a high affinity conformation, the balance between the two forms being defined by the allosteric constant L_0. In this study, influence of cholesterol- and caveolin-rich microdomains on NHE-1 activity was examined by using cholesterol depleting agents, including methyl-β-cyclodextrin (MBCD). These agents activated NHE-1 by modulating its L_0 parameter, which was reverted by cholesterol repletion. This activation was associated with NHE-1 relocation outside microdomains, and was distinct from NHE-1 mitogenic and hormonal stimulation; indeed MBCD and serum treatments were additive, and serum alone did not change NHE-1 localization. Besides, MBCD activated a serum-insensitive, constitutively active mutated NHE-1 (^{625}KDKEEEIRK^{635} into KNKQQQIRK). Finally, the membrane-dependent NHE-1 regulation occurred independently of Mitogen Activated Protein Kinases, especially Extracellular Regulated Kinase activation, although this kinase was activated by MBCD. In conclusion, localization of NHE-1 in membrane cholesterol- and caveolin-rich microdomains constitutes a novel physiological negative regulator of NHE-1 activity.
J. Cell. Physiol. 216: 207–220, 2008. © 2008 Wiley-Liss, Inc.

It is now well recognized that homeostasis of intracellular pH (pH_i) is an important modulator of numerous cell functions, notably through controlling enzyme activities and protein–protein interactions (Shrode et al., 1997). Among the pH_i-regulating mechanisms, an isoform of the Na^+/H^+ exchanger (NHE-1) expressed at the plasma membrane of all mammalian cells has been the most widely studied and is a key regulator of intracellular H^+ concentration upon acid loads (for reviews, see Counillon and Pouyssegur, 2000; Avkiran and Haworth, 2003). This exchanger uses the energy provided by the transmembrane sodium gradient to exchange one intracellular H^+ ion against one extracellular Na^+. It is nearly inactive at physiological pH_i but activates very steeply when the cytoplasm becomes acidic to reach full activity in less than one pH unit. This cooperative behavior constitutes an extremely efficient molecular switch for intracellular pH regulation. We have previously shown that this can be quantitatively explained by a Monod–Wyman–Changeux mechanism. Briefly, the transporter, which exists as a dimer in the plasma membrane, oscillates between a low and a high affinity form for intracellular protons (Lacroix et al., 2004). This balance, which is notably affected upon growth factor stimulation, is described by three constants: two affinity constants for intracellular protons and the thermodynamic constant associated with the allosteric transition (the ratio of the low affinity form to the high affinity form, L_0).

This exchanger also plays an essential role in cell volume regulation, and recent studies further imply it as an important actor of cell signaling, partly due to its properties as a scaffolding protein (Baumgartner et al., 2004; Bourguignon et al., 2004). In this context, any alteration of NHE-1 activity may lead to cell dysfunction, which might ultimately lead to the development of pathologies. For instance, NHE-1 activation has been related to

This article includes Supplementary Material available from the authors upon request or via the Internet at http://www.interscience.wiley.com/jpages/0021-9541/suppmat.

X. Tekpli and L. Huc equally contributed to the work.

L. Counillon and D. Lagadic-Gossmann equally supervised the work.

Contract grant sponsor: CNRS.
Contract grant sponsor: University of Nice-Sophia Antipolis.
Contract grant sponsor: Fondation de France, Programme Recherche Cardiovasculaire.
Contract grant sponsor: Institut National de la Santé et de la Recherche Médicale (INSERM).
Contract grant sponsor: Région Bretagne.
Contract grant sponsor: Ligue Nationale contre le Cancer.

*Correspondence to: Dominique Lagadic-Gossmann, Inserm U620, Université Rennes 1, Faculté de Pharmacie, 2 av Prof Léon Bernard, 35043 Rennes Cedex, France.
E-mail: dominique.lagadic@rennes.inserm.fr

Received 27 March 2007; Accepted 13 December 2007

DOI: 10.1002/jcp.21395

© 2008 WILEY-LISS, INC.

ischaemia/reperfusion alterations (Karmazyn, 1996), hypertrophy (Karmazyn, 2001), fibrosis (Young and Funder, 2003), and cancer (Cardone et al., 2005). Besides its role in proliferation processes, NHE-1 activation has also been reported to be part of apoptotic processes upon diverse stimuli (Khaled et al., 2001; Huc et al., 2004, 2007; Lagadic-Gossmann et al., 2004, 2007). In this context, how an NHE-1 activation of similar amplitude plays a role in such opposite processes remains to be elucidated and might stem from different regulation pathways, possibly resulting from differential phosphorylation (Khaled et al., 2001; Bourguignon et al., 2004; Mukhin et al., 2004), binding of modulators (Denker et al., 2000; Garnovskaya et al., 2003), or merely membrane characteristic changes (Bookstein et al., 1997).

In that respect, NHE-1 has been shown to be coupled to diverse membrane receptors, notably the G protein-coupled receptors or the growth factor receptors, whose activation triggers different protein kinase cascades leading to phosphorylation of NHE-1 C-terminal cytoplasmic domain (Counillon and Pouyssegur, 2000; Avkiran and Haworth, 2003). This latter domain is also capable of binding a number of proteins including calmodulin (Bertrand et al., 1994), calcineurin homologous proteins (Karmazyn, 1996), and phosphatase (Snabaitis et al., 2006) also involved in transporter regulation.

In the past few years, several data showed evidence that the biophysical properties of membrane bilayers have relevant effects on the properties of membrane proteins (Lee, 2004). NHE-1 is a transmembrane protein which is altered in lipid modification-related pathologies, such as atherosclerosis (Jung et al., 2004), cardiomyopathy (Okamoto et al., 1994; Karmazyn, 2001), diabetes (Lagadic-Gossmann et al., 1988; Battisti et al., 2003), and cancer (Barclay et al., 1955; Cardone et al., 2005). However, few studies have considered the influence of membrane lipids on its activity. Membrane fluidity has been identified as one such modulator (Bookstein et al., 1997; Gorria et al., 2006). Recently, we have obtained evidence that osmotic regulation modifies the allosteric balance of NHE-1 and that membrane curvature and/or tension would by itself modulate NHE-1 (Lacroix et al., unpublished work). Besides fluidity, plasma membrane is also characterized by its microstructure, more particularly by the presence of cholesterol-rich microdomains which have been notably implicated in the regulation of ion channels and transporters such as NHE-3 (Li et al., 2001; Murtazina et al., 2006). Regarding NHE-1, this protein has been recently found to be mainly located in caveolin-rich membrane microdomains, both in NHE-1-overexpressing cell models and in more physiological models, that is, when the endogenous protein is present at low levels (Bullis et al., 2002; Bourguignon et al., 2004; Willoughby et al., 2005). However, despite the fact that Bullis et al. (2002) found an alteration of NHE-1 membrane distribution upon methyl-β-cyclodextrin (MBCD, an agent commonly used for destabilizing cholesterol-rich microdomains by sequestering cholesterol), up to now, no study has thoroughly evaluated the role of membrane microdomains in the regulation of NHE-1 allosteric balance in the presence or not of mitogenic stimulation.

The present study clearly shows that destabilizing membrane microdomains by depleting membrane cholesterol both alters NHE-1 membrane microdistribution and activates the Na^+/H^+ exchange. Moreover, these two phenomena are reverted by cholesterol repletion of membrane and occur independently of prior mitogenic stimulation of the transporter.

Materials and Methods

Chemical reagents

MBCD, β-cyclodextrin (BCD), cholesterol, tetrarhodamine isothiocyanate (TRITC)-conjugated anti-rabbit IgG and the MKK1 inhibitor PD98059 were purchased from Sigma Chemicals Co (St Louis, MO). Cholesterol oxidase (CholOx), whose stock solution was dissolved in dimethyl sulfoxide (Me_2SO) and stored at −20°C, was purchased from Calbiochem (France Biochem, Meudon, France). Rabbit polyclonal anti-NHE-1 antibody (N1P1) was raised against a fusion protein encoding the last 157 amino acids of the human NHE-1 C-terminus (Sardet et al., 1990). Goat polyclonal anti-CD71 was purchased from Santa Cruz Biotechnology (Tebu-bio SA, Le Perray en Yvelynes, France). Secondary antibody conjugated to horseradish peroxidase was from Dako A/S (Glostrup, Denmark). Vybrant® Alexa Fluor® 488 Lipid Raft Labeling Kit and fluorescein phalloidin were purchased from Molecular Probes (Invitrogen, Cergy Pontoise, France).

Cell culture and transfection

Exchanger-deficient fibroblasts, PS120 cells (Pouyssegur et al., 1984), were grown as described by Touret et al. (2001). Transfections were performed using Fugene 6 (Roche, Meylan, France). Cell populations stably expressing the mutants were selected, using 500 μg/ml G418.

Semi-confluent monolayers on plastic dishes or glass coverslips were serum-depleted for 12–16 h before treatment. Serum-starved cells or cells exposed to Fetal Calf Serum (FCS, 20%; 20 min) were then treated for 5, 20, and 60 min with MBCD (2 mM), 10 min for CholOx (0.1 U/ml) in Cell Suspension Buffer (CSB, Huc et al., 2004) at 37°C. When cholesterol repletion was tested, cells treated with 2 mM MBCD during 20 min were washed with PBS and exposed to a mix of 40 μM cholesterol and 2 mM MBCD in Hepes-buffered solution at 37°C during 20 min. When using the MKK1 inhibitor, cells were pre-treated for 1 h with the inhibitor or the vehicle (DMSO at a final concentration <0.2%) and then co-treated with MBCD.

Site-directed mutagenesis

The amino acid sequence ^{625}KDKEEEIRK^{635} located at the C-terminal domain of NHE-1 and characterized by the presence of eight charged residues, was changed into KNKQQQIRK and called CTER+. This was performed using double-stranded mutagenesis (Quickchange site-directed mutagenesis, Stratagene). The different steps were performed as described by Poet et al. (2001), using oligonucleotides bearing the appropriate codon changes and minimizing the possible mismatches (MWG Biotech) on a 1.6 kb *Sac*I—*Eco*RI DNA cassette containing the sites of interest. After sequencing, the mutated cassette was reintroduced by restriction cutting and subsequent religation in the modified polycistronic pECE-IRES vector (SV40 promoter) containing the NHE-1 cDNA (Lacroix et al., 2004). The presence of the mutations was again checked by automated sequencing (GenomeExpress). The R327E substitution, which stabilizes the transporter in the low-affinity conformational state of the allosteric mechanism, has been previously described (Lacroix et al., 2004).

Measurement of initial rates of Na^+/H^+ exchange

NHE-1-stably transfected PS120 were seeded in 24-well plates. The cells were then serum-starved for at least 12 h before the experiments. Prior to acidification, cells were treated for 5 min with the different agents (0.1 U/ml CholOx, 2 mM MBCD, the 2 mM MBCD—40 μM cholesterol mix, or 2 mM BCD). They were then incubated for 5 min in sodium-free solutions containing 2.5 μM nigericin (Sigma), 140 mM KCl, the pH was adjusted in the range of 5.6–6.8 in the presence of 20 mM of Hepes, MOPS, or MES buffers. Nigericin was then scavenged by a 5-min incubation in the same solutions in which nigericin was replaced by 50 mg/ml BSA. The cells were then rinsed twice in sodium free medium (120 mM Choline Chloride, 1 mM $CaCl_2$, 1 mM $MgCl_2$, 5 mM Glucose, buffered at pH 7.0 with 10 mM Hepes). Linear sodium uptake was carried out for 15–30 sec in the same medium containing

0.25 μci/ml $^{22}Na^+$, at a final Na^+ tracer concentration of 0.5 mM. Uptake was stopped by four rapid rinses in ice-cold phosphate buffered saline (PBS). Cells were solubilized in 0.1 N NaOH and radioactivity was measured by scintillation-counting. NHE-1 initial rates were calculated as the cariporide (10 μM)-sensitive $^{22}Na^+$ accumulations, which were in the order of magnitude of a few thousand counts per minute at the plateau. Growth factor activation was measured by addition of 20% FCS 10 min before the acidification. Na^+/H^+ exchange activity in the absence of growth factors was measured on serum-starved cells for 12 h. To reach maximal velocities, two wells per experiment were acidified using the NH_4^+ pre-pulse technique, using a 1-h incubation in 50 mM NH_4Cl, 70 mM Choline chloride, 5.4 mM KCl, $CaCl_2$ 1 mM, $MgCl_2$ 1.2 mM, Glucose 5 mM, buffered at pH 7.4 with 10 mM Hepes, either in the presence or not of MBCD. Cells were then rinsed in 120 mM Choline Chloride, 1 mM $CaCl_2$, 1 mM $MgCl_2$, 5 mM Glucose, buffered at pH 7.0 with 10 mM Hepes. Under these conditions, intracellular pH dropped to the estimated value of 5.2 (see below). Initial rates of $^{22}Na^+$ uptake were then measured as described above.

Intracellular pH measurements

The pH_i of PS120-NHE-1 cells was monitored using the pH-sensitive dye BCECF/AM (2′,7′-bis(carboxyethyl)-5-6-carboxyfluorescein/Acetoxy Methylester; 5 μM). Cells were incubated for 60 min with 50 mM NH_4Cl, 90 mM NaCl, 5.4 mM KCl, 1 mM $CaCl_2$, 1 mM $MgCl_2$, 5 mM Glucose, buffered at pH 7.4 with 10 mM Hepes, and treated or not with 2 mM MBCD for 5 min. To start the acidification, cells were next rinsed with a Na^+-free 120 mM Choline Chloride Hepes-buffered solution. Once a steady-state acid level was reached, pH_i recovery was then triggered by replacing Choline Chloride by NaCl.

During all these steps, which were performed at room temperature, pH_i variations were monitored by the measurement of BCECF/AM fluorescence. The imaging system consisted of a Zeiss ICM 405 inverted microscope with a Zeiss 40X objective, coupled to a video camera. Fluorescence excitation was provided by a 75 W Xenon lamp (Osram), and was computer-controlled by a shutter. The excitation beam was filtered through 450 and 490 nm narrow band interference filters paired with appropriate quartz neutral-density filters mounted in a computer-controlled motorized wheel. Therefore, the cells were excited successively at 490 and 450 nm, and each image was digitized and stored on the computer hard disk. Image treatment was performed using the Axon^R Imaging Workbench (AIW 4.0) software.

At the end of each experiment, the fluorescence signals relative to pH_i were calibrated using the K^+/H^+ exchanging ionophore nigericin. For this purpose the cells were successively perfused with KCl solutions (140 mM KCl, 20 mM Hepes, and 10 μM nigericin) adjusted to pH 7.6, 7.0, and 6.0. The pH_i values were then calculated from the gray level values using the $pH = 6.8 + \log(R - R_{min}/R_{max} - R)$ equation. These values were then adjusted according to the experimental calibration using linear interpolation. For the most acidic pH_i values obtained from ammonium acid load experiments, these were estimated using non-linear interpolation of the compilation of nine nigericin calibration curves for pH_i values ranging from 7.8 to 5.8.

Purification of cholesterol-rich microdomains

After treatment, cells were washed twice with ice-cold PBS, lysed in 1 ml buffer MBS-buffered saline [25 mM 2-(*N*-morpholino)ethanesulfonic acid (pH 6.5), 150 mM NaCl, and complete protease inhibitor mixture, Sigma] containing 1% Triton X-100 for 30 min at 4°C before passing them through an ice-cold cylinder cell homogenizer. Lysates were then diluted with 2 ml MBS buffer containing 80% sucrose (w/v) and placed at the bottom of a linear sucrose gradient consisting of 8 ml 5–40% sucrose (w/v) in MBS. Samples were centrifuged at 39,000 rpm using a Beckman SW41Ti rotor for 20 h at 4°C, and 11 fractions of 1-ml each were collected from the top of the gradient, and proteins were quantified according to the Lowry method (Biorad, Marnes la Coquette, France).

In order to validate the results obtained when applying the detergent protocol, a conventional detergent-free method (Song et al., 1996) was also used for isolation of cholesterol-rich membrane microdomains. Triton X-100 was thus replaced with sodium carbonate buffer 0.5 M, pH = 11, completed with protease inhibitor mixture (Sigma). Homogenization was carried out sequentially by using a 23 G needle (15 strokes), then an ice-cold cylinder cell homogenizer (10 strokes), and finally a sonicator (three 20 sec bursts). Lysates were then treated as described above.

Immunostaining

PS120 cells were seeded into 35 mm dishes on glass coverslips and treated. After washing in PBS, adherent cells were fixed on coverslips with 4% paraformaldehyde in PBS for 20 min at 4°C and washed three times with PBS. Then, cells were incubated for 30 min with a blocking-permeabilizing solution (0.2% saponin-2% BSA in PBS). After washing, cells were incubated with rabbit anti-NHE-1 primary antibody in a blocking-permeabilizing solution for 2 h at room temperature, washed in PBS and then stained with TRITC-conjugated anti-rabbit IgG for 1 h at room temperature. Vybrant® Alexa Fluor® 488 Lipid Raft Labeling Kit to stain ganglioside GM1, and fluorescein phalloidin to stain F-actin were used following instructions provided by the manufacturer. Thereafter, cells were co-stained by a 15-min incubation in a blocking solution containing 1 μg/ml DAPI, a fluorescent dye specific for DNA. After washing, coverslips were mounted with PBS-glycerol-Dabco. Fluorescence-labeled cells were captured with a Leica Confocal microscope (Leica Microsystemes SAS, Rueil-Malmaison, France) or with a DMRXA Leica microscope and a COHU high performance CCD camera, using Metavue software. Data are representative of at least three independent experiments.

Cholesterol analysis of lipid raft fractions

Lipids were extracted using the method of Folch (Folch et al., 1957). Cholesterol concentrations in detergent-resistant (DR) (i.e., cholesterol-rich fractions) and soluble (S) fractions were measured using the colorimetric method Infinity™ cholesterol (ThermoTrace, Melbourne, Australia), following instructions provided by the manufacturer. Absorbance of samples was measured at 492 nm on a microplate reader (Multiscan, Labsystems, Cergy Pontoise, France). Cholesterol concentration was expressed in μM/μg proteins.

Alkaline phosphatase activity assays

Alkaline phosphatase activity was determined as previously reported (Parkin et al., 1999; Eckert et al., 2003). Briefly, 100 μL of sample was incubated with an equal volume of *p*-nitrophenylphosphate solution (Sigma). After 20 min of incubation at 37°C, the absorbance was read at 405 nm using a microplate reader (Multiscan, Labsystems) and levels of *p*-nitrophenol production were calculated using a standard curve.

Western blot analysis

Following cell lysis (CytoBuster™ Protein Extraction Reagent, Calbiochem) or purification of cholesterol-rich domain fractions, proteins were subjected to electrophoresis as previously described (Huc et al., 2004). Relative amounts of proteins were ascertained by Ponceau S red staining of the membranes. The primary antibodies used for MAPK detection were: anti-human phospho-p38 MAPK [Thr180/Tyr182], anti-phospho-ERK 1 and 2 [Thr202/Tyr204], and anti-ERK 1/2 antibodies, all provided by New England BioLabs (Beverly, MA); anti-phospho-JNK [Thr183/Tyr185] and anti-JNK antibodies provided by Cell Signaling

(Ozyme, St. Quentin-en-Yvelynes, France) and Calbiochem, respectively; anti-mouse p38 antibody [p38 (C-20); Santa Cruz Biotechnology; TEBU, Le Perray-en-Yvelines, France].

For analysis of plasma membrane NHE-1 expression, 20 μg of membrane proteins prepared from PS120 cells transfected with WT NHE-1s were run on 7.5% acrylamide gels (Biorad mini gel system). Immunoblots were carried out as described by Counillon et al. (1994), using a commercial monoclonal antibody against the NHE-1 C-terminal end (Chemicon, Millipore, France). Semi-quantitative analysis was performed on both NHE-1 mature and non-mature form using densitometric analysis relative to F-actin (Calbiochem antibody) with the ImageJ software (Rasband, W.S., ImageJ, U. S. National Institutes of Health, Bethesda, Maryland, USA, http://rsb.info.nih.gov/ij/, 1997–2007).

Trypsin accessibility assay

The presence of the mature form of NHE-1 at the plasma membrane was determined by exposing the cells for 60 sec to extracellularly-applied trypsin (Invitrogen BRL) at 0.5 mg/ml in PBS at room temperature. Cells were then rinsed twice with ice-cold PBS supplemented with 5% BSA. Crude Membranes were then prepared as described in Counillon et al. (1994). The different forms of NHE-1 (mature, cleaved and non-mature), either in control conditions or following MBCD treatment, were visualized by western-blotting as described above.

Data analysis

Data were fitted using Sigmaplot 2001 (Jandel) with built-in or user-defined equations as described previously (Lacroix et al., 2004). The experimental data points (with standard errors of the mean SEM) correspond to the compilation of at least three independent experiments, with each experimental data point determined at least in duplicate. Constants obtained from fitting our data are provided with the error of the fits and r^2 goodness-of-fit factors.

Results

Methyl-β-cyclodextrin and cholesterol oxidase, two known destabilizing agents of lipid microdomains, modify NHE-1 activity by modulating the allosteric equilibrium

The first set of experiments was carried out in order to test the effects of membrane microdomain alterations by cholesterol depletion on NHE-1 cooperative regulation in PS120 fibroblasts stably expressing NHE-1 (Pouyssegur et al., 1984). To this aim, cells were exposed for 5 min to either MBCD (2 mM) (Kilsdonk et al., 1995) or CholOx (0.1 U/ml) (Gadda et al., 1997), at different intracellular pH values. Rapid uptakes of $^{22}Na^+$ were then measured in Hepes-buffered solutions (to avoid any participation of the HCO_3^--dependent pH_i regulating mechanisms). This ensures initial rate measurements and thus allows the steady-state determination of the kinetic parameters of Na^+/H^+ exchanger NHE-1 expressed in the PS120 fibroblasts (Lacroix et al., 2004), in response to acidifications and to changes in membrane microstructure. As illustrated in Figure 1A, cell exposure to MBCD resulted in NHE-1 activation as evidenced by the leftward shift of the sigmoidal activity curve of NHE-1 measured at different intracellular pH. No significant variations of maximal rates of NHE-1 were detected under these conditions (Fig. 1D). We independently quantified NHE-1 activity by measuring pH recoveries using BCECF fluorescence after an acidification induced by NH_4Cl pre-pulse. As shown in Figure 1C for averaged data (and also in Supplementary Fig. 1A for representative pH_i recordings), the exposure to MBCD resulted in an enhanced NHE-1 mediated pH recovery, above pH values of about 6.0–6.5, thus confirming the above observations. The values of the pH recovery slopes in the acidic pH_i range [5.6–6.2] were compiled and, although the MBCD treatment might provide a slightly higher slope value, no significant difference was observed (see inset, Fig. 1C). This indicates that the maximal rate of the transporter is not modified by cholesterol depletion and provides an independent confirmation to our results obtained by $^{22}Na^+$ uptake measurement (Fig. 1D).

In order to ensure the specificity of MBCD treatment toward membrane cholesterol, a cholesterol repletion protocol was applied; so, following exposure of cells to MBCD, cells were exposed for 20 min to 2 mM MBCD supplemented with 40 μM cholesterol. As shown in Figure 1A, such a maneuver prevented the activation of NHE-1 upon MBCD exposure. Note also that medium enrichment with cholesterol in the absence of any prior depletion led to a rightward shift of the activation curve of NHE-1, thus indicating a negative allosteric regulation of the exchanger.

The data were fitted using the Monod–Wyman–Changeux equation, which describes NHE-1 allosteric regulation by intracellular protons (Lacroix et al., 2004), taking either the L_0 allosteric constant or the microscopic affinities for protons as variables. We found that MBCD treatment fitted best with decrease in L_0 (also observed with CholOx: $L_0 = 5952 \pm 513$ vs. 975 ± 52, $n = 3$, control vs. CholOx, respectively), rather than with a change in the microscopic affinity constants of the system which gave poor fits with our data. Such a decrease was inhibited by repletion of cholesterol. In contrast, treatment with cholesterol alone fitted with a marked increase of L_0. Altogether these results clearly show positive and negative regulation of NHE-1 by cholesterol depletion and enrichment, respectively, which are due to the modulation of the allosteric constant of the transporter (Fig. 1B).

Treatments with methyl-β-cyclodextrin or cholesterol oxidase alter ganglioside GM1 membrane localization, but not NHE-1 plasma membrane expression

In order to test the effects of MBCD and CholOx on cholesterol-rich membrane microdomains, we stained PS120-NHE-1 cells for ganglioside GM1, using FITC-coupled cholera toxin which specifically binds to this lipid. Figure 2A shows that, under control conditions, cells exhibited a punctuate pattern for GM1 staining, which may correspond to the cholesterol- and GM1-rich microdomains. Upon cell treatment with the cholesterol-depleting agents, a disruption of these microdomains was observed, with a more diffuse pattern for GM1 staining at the plasma membrane, thus proving the efficacy of both treatments for altering membrane microstructure in our cell model. To study the NHE-1 plasma membrane localization, we co-stained the PS120-NHE-1 fibroblasts with both an antibody against NHE-1 and fluorescein phalloidin to detect F-actin. As shown in Figure 2B, both MBCD and CholOx did not disturb NHE-1 plasma membrane localization as NHE-1 remained perfectly co-localized with F-actin. This was confirmed by analyzing the expression of the NHE-1 mature form at the plasma membrane. This was performed by trypsin accessibility assays as well as by densitometric analysis. Following a 60-sec-cell exposure to extracellularly-applied trypsin, only the mature NHE-1 inserted in the plasma membrane is known to be cleaved. As shown in Figure 2C,D, MBCD did not elicit any changes in the total amounts of the trypsin-sensitive NHE-1 inserted in the plasma membrane.

Taken together with the kinetic data shown in Figure 1, these data indicated that cholesterol depleting agents were responsible for an increase in the gain of NHE-1 cooperative activation by intracellular protons, without any change in the protein expression at the plasma membrane. However, based upon the fact that both these agents were shown to disturb microdomains in our cell model (as visualized by GM1 staining),

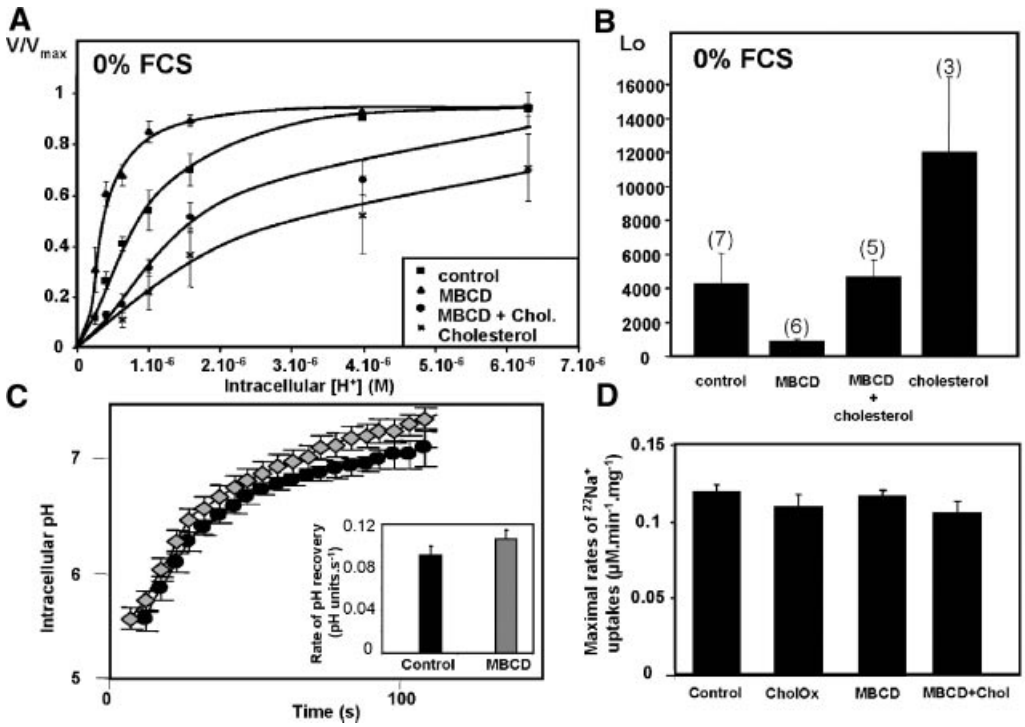

Fig. 1. Modulation of NHE-1 activity by cholesterol in the absence of growth factors. A: PS120-NHE-1 cells were seeded in 24-well plates and maintained in 0% FCS during 16–18 h prior to acidifications at different intracellular pH values using the nigericin technique as described in Lacroix et al. (2004). Activities of NHE-1 were determined by measuring fast $^{22}Na^+$ uptakes conducted after treatments aimed at modifying cholesterol membrane content as described in Materials and Methods Section. ■: Control conditions, ▲: 5 min exposure to 2 mM MBCD, ●: 5 min exposure to 40 μM cholesterol following 20 min exposure to MBCD. ×: direct addition of 40 μM cholesterol. Plots represent V/V_{max} values as a function of intracellular H^+ concentration. The error bars correspond to SEM. Note the increase in NHE-1 cooperative response upon cholesterol depletion and its decrease upon cholesterol addition. B: Modulation of NHE-1 allosteric constant (L_0) by cholesterol. Allosteric constants were calculated from the experimental data presented in part (A) using the Monod–Wyman–Changeux equation for a dimeric NHE-1 as described in Materials and Methods Section. The number of independent experiments is provided in the figure. The data are quoted as means ± standard error of the mean. The values presented correspond to goodness of the fit factors (rsq) higher than 0.9. Note that an increase in the value of L_0 corresponds to an allosteric inhibition of the transporter. C: Comparison of averaged intracellular pH variations in acidified fibroblasts treated or not with MBCD. Dark: control conditions, gray: MBCD treatment. NHE-1 transfected fibroblasts were acidified using a NH_4Cl (50 mM; 1 h) pre-pulse. pH recoveries were measured using BCECF fluorescence. Inset: effect of MBCD on the slopes measured at the acidic pH range of [5.6–6.2]; note that no significant difference was observed. N = 5 independent experiments with 16 cells measured in each experiment. Error bars are SEM. D: Compilation of the maximal velocities measured as initial rates of cariporide-sensitive $^{22}Na^+$ uptake in NHE-1 transfected fibroblasts. The different bars of the histogram correspond either to control conditions or to fibroblasts treated with CholOx, MBCD, or MBCD plus 40 μM cholesterol, as described in Materials and Methods Section.

we next supposed that the NHE-1 cooperative regulation presently detected might be related to the protein localization into or outside microdomains.

Methyl-β-cyclodextrin or cholesterol oxidase alter the distribution of NHE-1 between different membrane domains in PS120-NHE-1 fibroblasts

In order to gain further insight into the effects of cholesterol depleting agents on NHE-1 membrane distribution, both control and treated cells were exposed to Triton X-100 at 4°C and lysates were then centrifuged on a sucrose gradient in order to get DR (which correspond to cholesterol-rich membrane microdomains) and soluble fractions (S; which correspond to the more fluid part of the membrane). Aliquots from each of the 11 fractions collected from the gradients were then analyzed by western blotting for the presence of caveolin-1 (cav 1), or transferrin receptor CD71 (a known marker of S fractions). As shown in Figure 3A, cav 1 expression was detected in fractions 2–6, whereas CD71 was found in fractions 8–11. The DR fractions were further characterized by a high concentration of cholesterol, and a high activity of alkaline phosphatase, as compared to S fractions. So DR fractions were distributed from 1 to 7 whereas 8 to 11 fractions define S fractions. The same observations were made when applying a detergent-free protocol to isolate cholesterol-rich microdomains (see Supplementary Fig. 3). The efficacy of MBCD to alter membrane microstructure was confirmed by showing a significant decrease (by about 40%) of cholesterol concentration in pooled DR fractions (1–7; Fig. 3B), as soon as a 5-min treatment with 2 mM MBCD, as well as a redistribution of caveolin-1 expression (Fig. 3C,D). Similar effects were observed with a 10 min-treatment with CholOx. We also used BCD (2 mM, 1 h) to compare the effects of this compound to those induced by MBCD. As shown in Figure 3B, no effect of BCD on cholesterol concentration was observed, thus confirming the specificity of MBCD action on cholesterol.

Regarding NHE-1 distribution, as illustrated in Figure 4A, our data clearly show the preferential localization of the protein in DR fractions (since only 2 μg of proteins were loaded on gels for fractions 1–7, compared to 200 μg for fractions 8–11). As clearly shown in Figure 4B, the detergent protocol used for microdomain isolation was not responsible for the observed distribution of NHE-1 since similar effects were also detected

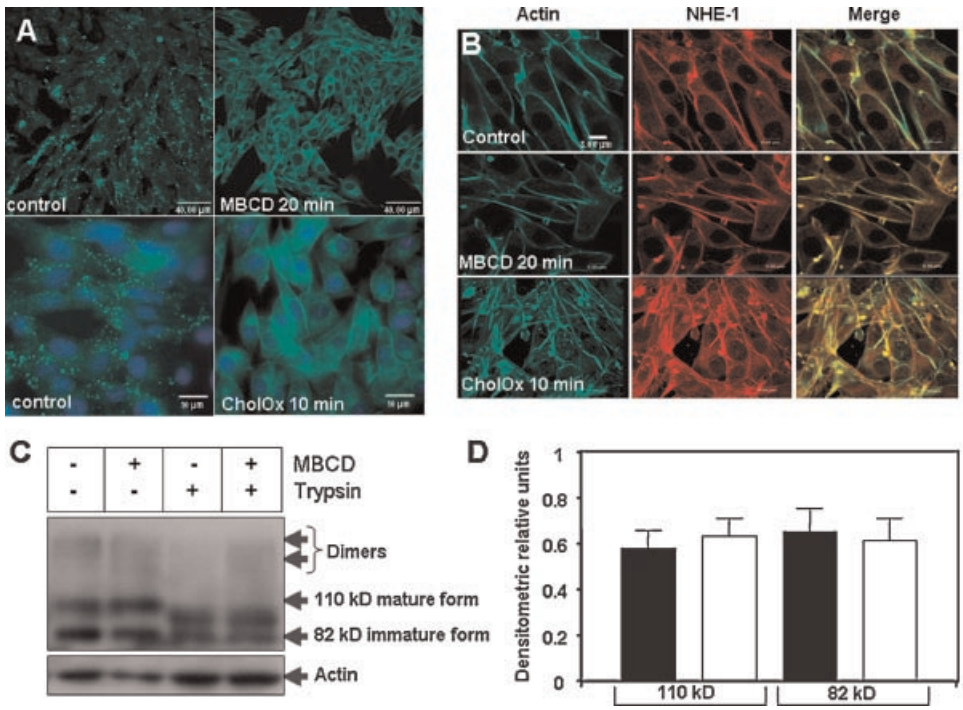

Fig. 2. Treatments with methyl-β-cyclodextrin or cholesterol oxidase alter ganglioside GM1 membrane distribution, but not NHE-1 plasma membrane expression. PS120-NHE-1 cells were treated or not with 2 mM MBCD or with 0.1 U/ml CholOx for 1 h or 10 min, respectively. A: After fixation and permeabilization, immunostaining of cells was performed with Alexa 488 conjugated-cholera toxin subunit B (to visualize GM1 ganglioside; green), followed by an incubation of an anti-Cholera toxin subunit B antibody for crosslinking. Cells were viewed by confocal fluorescence microscopy (MBCD) or fluorescence microscopy (CholOx). B: After fixation and permeabilization, immunostaining of cells was performed with a rabbit polyclonal anti-NHE-1 antibody and fluorescein phalloidin to visualize F-actin (green), and with an anti-rabbit antibody coupled to TRITC (red). Cells were viewed by confocal fluorescence microscopy (magnification 400×). Co-localizations are seen in yellow. The experiments were repeated at least three times, with similar results. C: Comparison of the quantities of NHE-1 at the plasma membrane measured under control conditions or following a MBCD treatment. Trypsin accessibility assay: the presence of the mature form of NHE-1 at the plasma membrane was determined by exposing the cells for 60 sec to extracellularly-applied trypsin. Under these conditions, only the NHE-1 inserted in the plasma membrane is cleaved. Trypsin action was then stopped by two rinses (10 sec) with ice-cold PBS supplemented with 5% BSA. Total membranes were prepared as described in Materials and Methods Section. The different forms of NHE-1 (mature, cleaved and non-mature), either in control or following MBCD treatment, were visualized by western-blotting. D: Semi-quantitative estimation of the amounts of plasma membrane NHE-1 following MBCD treatment (white) compared to control conditions (black). After 15 min treatment with MBCD, total membranes were prepared. Mature and non-mature NHE-1 form amounts were estimated using densitometric analysis after western blotting. The histogram presented corresponds to the compilation of eight independent determinations. Data were normalized using actin as an internal standard. Error bars are SEM. [Color figure can be viewed in the online issue, which is available at www.interscience.wiley.com.]

using the detergent-free protocol. Furthermore, a 1-h treatment with MBCD (2 mM) resulted in the disappearance of NHE-1 expression from DR fractions; similar effects were observed following a 10-min treatment with CholOx. As shown in Figure 4C, western blotting performed on pooled DR or S fractions (5 and 100 μg of proteins loaded for DR and S, respectively) indicated that MBCD treatment was already efficient on redistributing NHE-1 as soon as 5 min. Our results also showed that CholOx, known to oxidize cholesterol, was more efficient than MBCD to induce alterations in NHE-1 redistribution, since a 10-min treatment with this compound was as efficient as a 1-h treatment with MBCD. From Figure 4A,C, it was clear that, upon both MBCD and CholOx, NHE-1 was redistributed from cholesterol-rich microdomains to the more fluid membrane domains; indeed, an increase of NHE-1 concentration in the S fraction was observed simultaneously to the decrease in DR fraction. Note also that a similar effect of MBCD was observed when applying the non-detergent protocol (Fig. 4B). Finally, cholesterol repletion following a 20-min treatment with MBCD prevented NHE-1 redistribution, even inducing a slight increase of NHE-1 expression in DR fractions (Fig. 4D). This therefore points to a direct role for cholesterol in maintaining NHE-1 in caveolin-rich membrane microdomains, thereby negatively regulating the exchanger. Note that a 1-h treatment with BCD neither reduced NHE-1 expression in DR fractions (Fig. 4E), nor affected NHE-1 activity (see Supplementary Fig. 1).

Altogether, these results demonstrated that cholesterol modulated both cooperative regulation of NHE-1 and its localization into cholesterol-rich domains.

These effects are independent and additive to that of growth factor stimulation

In order to examine whether the modulation of NHE-1 by growth factors or by microdomain alterations used the same pathways or were simply independent and additive, we next characterized NHE-1 response to MBCD after 20 min of stimulation with 20% serum. As shown in Figure 5A, this treatment resulted in a leftward shift of the sigmoidal activation curve of NHE-1. Such an effect was accompanied by a twofold decrease of the L_0 parameter (Fig. 5B). Like in the absence of serum, repletion of cell membrane with cholesterol reverted

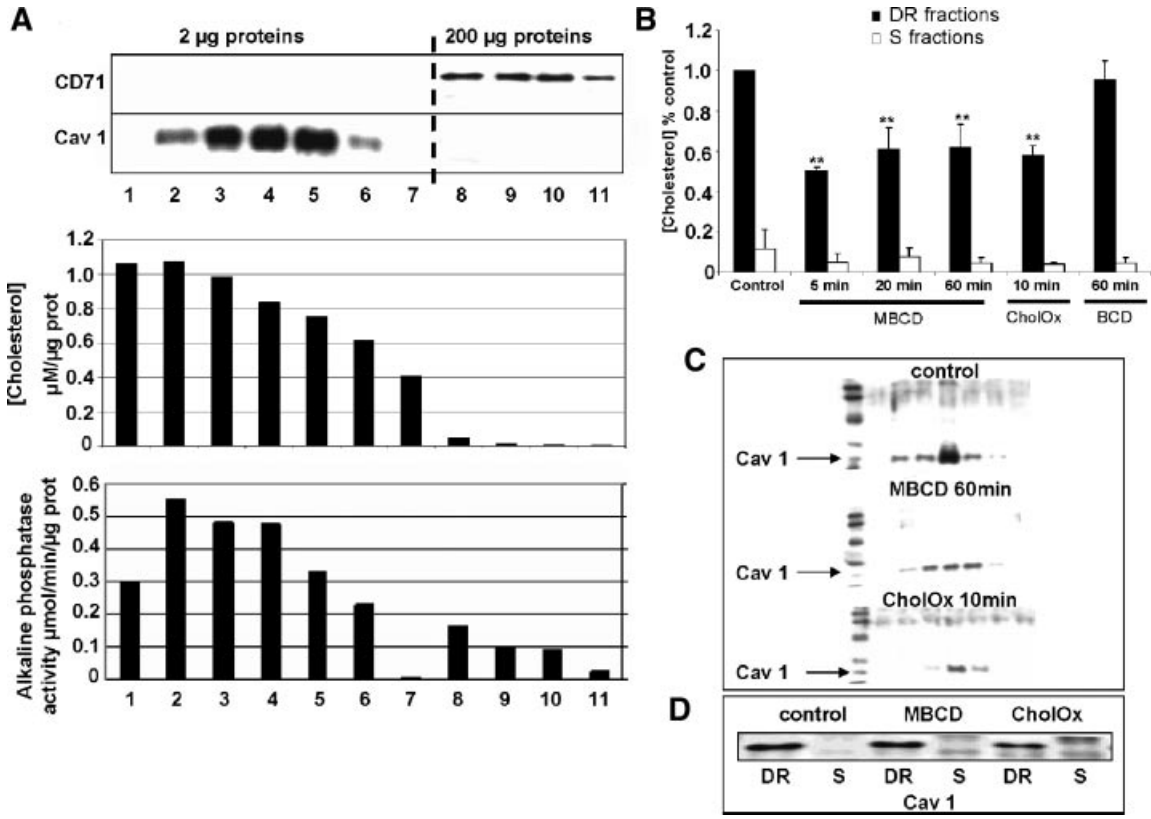

Fig. 3. MBCD and CholOx affect characteristics of membrane microdomains in PS120 cells. Membrane microdomains were isolated as described in Materials and Methods Section, from PS120-NHE-1 cells, either untreated (A–C), treated with 2 mM MBCD during 5, 20 (B) and 60 (B,C) min, with 0.1 U/ml CholOx during 10 min (B,C), or with 2 mM BCD during 60 min (B). A: Characterization of membrane microdomains in PS120-NHE-1. For western blot analysis of caveolin 1 and CD71 distribution following cholesterol-rich domain isolation, 2 and 200 µg were loaded for fractions 1–7 and 8–11, respectively. Histograms are showing cholesterol content and alkaline phosphatase activity (as described in Materials and Methods Section) corresponding to the 11 fractions. B: Estimates of cholesterol content in pooled detergent resistant (DR; 1–7) and soluble (S; 8–11) fractions following MBCD, CholOx, BCD treatments, expressed in % versus control. Data are given as means ± SEM (n = 3–5). **$P < 0.01$, t-test, MBCD versus control. C: Western Blot analysis of caveolin 1 distribution in DR fractions after MBCD and CholOx exposures. Two microgram of proteins were loaded for each fraction. D: Western Blot analysis of caveolin 1 distribution in DR and S fractions after MBCD and CholOx esposures; 5 and 100 µg of the DR (1–7) and S fractions (8–11) were loaded, respectively. Data were representative of at least three independent experiments.

the effects of MBCD whereas enrichment of medium with cholesterol led to a significant inhibition of NHE-1 activity (Fig. 5A,B). Therefore, whether NHE-1 was activated by serum or not, NHE-1 still responded to MBCD. These results thus clearly indicated that the cooperative regulation of NHE-1 by mitogens and that by cholesterol membrane content occurred independently to each other and were additive. Note that, as expected, a lower L_0 was detected in the presence of serum (Fig. 5B) compared to serum-free conditions (Fig. 1B).

Like in the absence of serum, a disruption of GM1-microdomains was observed upon MBCD treatment of serum-treated cells (Fig. 6A). Furthermore, when looking at the NHE-1 expression at the plasma membrane in these cells, we observed that such a compound did not alter NHE-1 co-localization with F-actin (Fig. 6B), although a decrease of NHE-1 expression in DR fractions along with an increase in S fractions was detected (Fig. 6C). Besides, it is noteworthy that the presence of FCS alone did not modify NHE-1 distribution between DR and S fractions.

Therefore, these data suggest that the regulation of NHE-1 by mitogens and cholesterol membrane content rely upon independent molecular pathways.

Methyl-β-cyclodextrin is capable of activating NHE-1 in R327E and the constitutively active CTER+ mutants

In order to gain further insight into the modulation of NHE-1 allosteric balance by cholesterol depleting agents, we decided to test their effects on two NHE-1 mutants: the R327E mutant for which the R327E substitution stabilizes the transporter in the low-affinity conformational state of the allosteric mechanism (Lacroix et al., 2004), and the CTER+ mutant for which the mutation of three glutamate residues (see Materials and Methods Section) results in a constitutively active form of NHE-1, that is consequently poorly sensitive to serum stimulation (Fig. 8C). As shown in Figure 7, such mutations per se neither affected cholesterol concentrations in DR fractions (part A), nor the overall NHE-1 distribution in membrane microdomains (part B), or its expression in pooled DR and S fractions (part C).

Analysis of NHE-1 expression in DR and S fractions after MBCD treatments (20 min) revealed a redistribution of the NHE-1 mutant form from DR to S fractions, whatever the mutant under consideration (Fig. 8A). Regarding NHE-1 activity, the R327E mutant was found to be sensitive to serum, although at a low level, as previously described (Lacroix et al.,

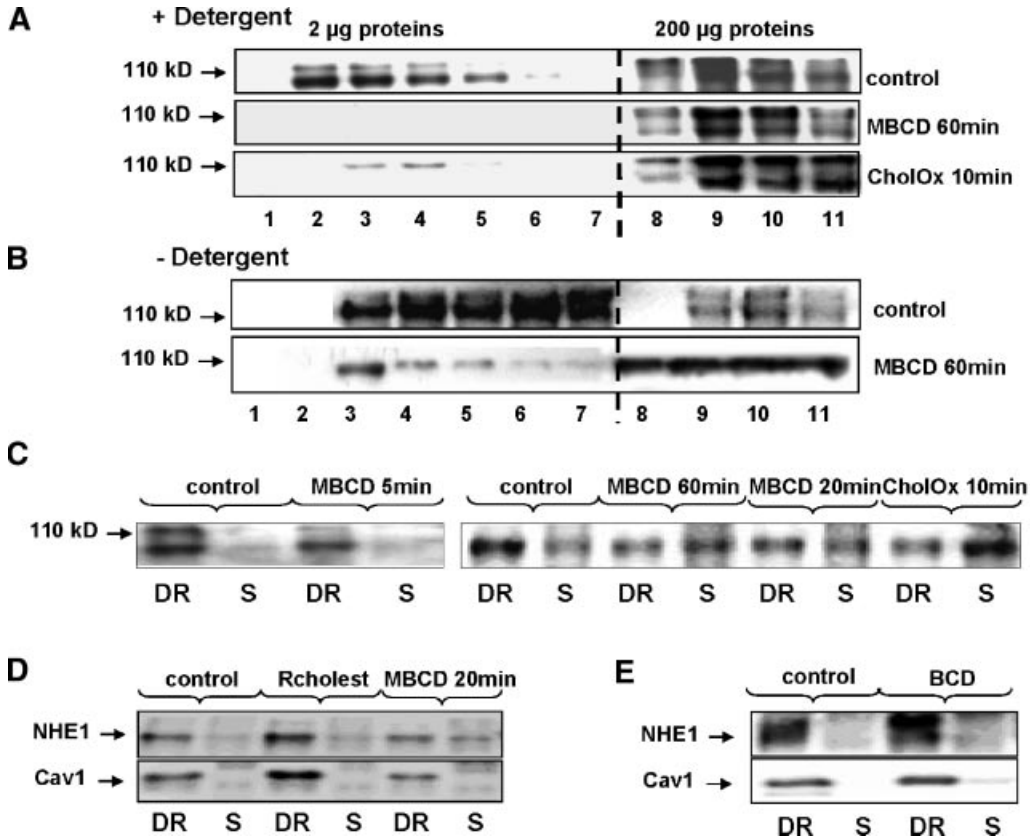

Fig. 4. MBCD and CholOx change NHE-1 membrane distribution. Membrane microdomains were isolated as described in Materials and Methods Section, from PS120-NHE-1 cells, either untreated (A–E), treated with 2 mM MBCD during 5 (C), 20 (C,D), and 60 (A–C) min, with 0.1 U/ml CholOx during 10 min (A,C), or with 2 mM BCD during 60 min (E), followed or not by cholesterol repletion (Rcholest: 40 µM cholesterol, 2 mM MBCD)(D). A,B: Western blot analysis of NHE-1 distribution following cholesterol-rich domain isolation using either a detergent (A) or a non-detergent (B) based protocol. Two and 200 µg were loaded for fractions 1–7 and 8–11, respectively. C–E: Western blot analysis of NHE-1 distribution on pooled detergent resistant (DR; 1–7: 5 µg) and soluble (S; 8–11: 100 µg) fractions. Data were representative of at least three independent experiments.

2004), and a further activation of the transporter was observed when cells were exposed to MBCD in the presence of 20% of serum (Fig. 8B,D). This particular behavior confirms that NHE-1 regulation by MBCD is due to a modulation of L_0 allosteric constant.

Regarding the CTER+ mutant, whereas the L_0 parameter of NHE-1 was barely affected by the presence of serum, a significant decrease of this parameter was nevertheless detected upon MBCD (Fig. 8C,D). This finding shows that a mutant which cannot be activated by canonical signaling pathways can be further activated by cholesterol depletion. This set of results provides a strong evidence for the existence of these two distinct regulating pathways for NHE-1.

Effects of methyl-β-cyclodextrin on NHE-1 activity are independent of ERK activation

NHE-1 has been shown to be regulated by Mitogen Activated Protein (MAP)-kinases, particularly ERK (Bianchini et al., 1997), p38 (Khaled et al., 2001), and JNK (Huc et al., 2007). Besides, MBCD has also been described to activate numerous kinases, including MAPKs (Furuchi and Anderson, 1998; Wang et al., 2005). We then decided to test whether MAPK pathways were involved in NHE-1 activation upon MBCD treatment. We first evidenced that, under our experimental conditions, ERK was rapidly phosphorylated in MBCD-treated cells, especially in the absence of FCS (Fig. 9A; note that in the presence of FCS, a basal ERK phosphorylation was already detected, as expected); besides, no further activation of p38 was observed as compared to control (Fig. 9B). Regarding JNK, no phosphorylated form was detected whatever the conditions tested (data not shown). Following the identification of ERK activation, we then performed inhibition experiments with PD98059 (PD, 20 µM), a well-known chemical inhibitor of MKK1/2, the kinases upstream ERK 1/2 (Dudley et al., 1995). Western blot in Figure 9A demonstrated that PD treatment prevented ERK phosphorylation induced by MBCD. However, measurements of NHE-1 activity at three different acid pH values showed no effect of ERK inhibition on the stimulation of $^{22}Na^+$ uptakes by MBCD, either in absence (Fig. 10A), or in presence of FCS (Fig. 10B). In this latter case, as expected, inhibition of ERK activation decreased control NHE-1 activity at pH_i 6.4. Thus, ERK activation following MBCD treatment was not responsible for NHE-1 activation.

Discussion

NHE-1 is a prominent pH_i-regulator, also involved in the regulation of cell volume, sodium homeostasis, proliferation/apoptosis balance, cell adherence and migration. . . If its regulation modalities by pH or by extracellular stimuli, such as mitogens or hormones, are quite well established (for review,

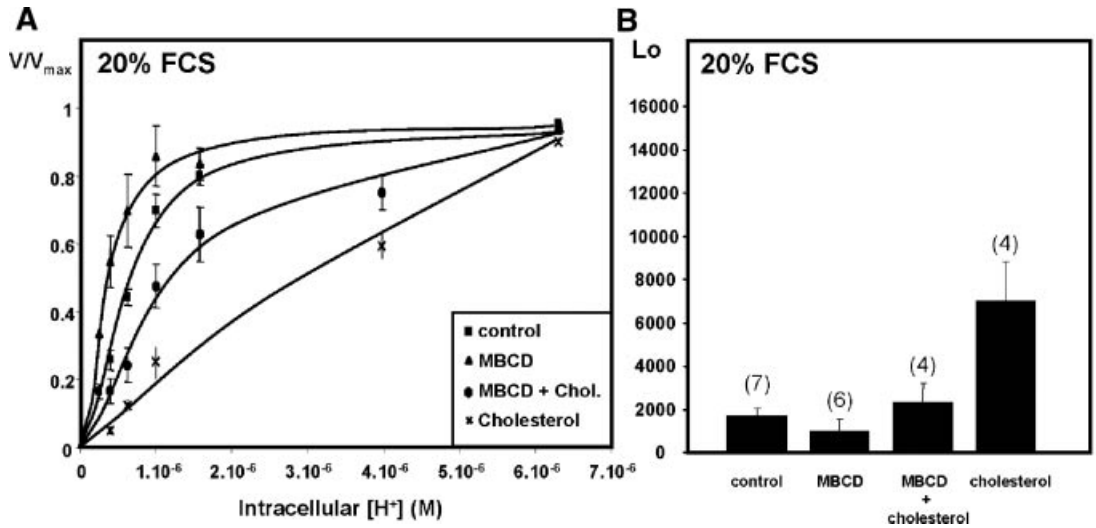

Fig. 5. Modulation of NHE-1 activity by cholesterol in the presence of growth factors. A: Activity of NHE-1 measured at different intracellular pH values. Cells expressing WT NHE-1 seeded in 24-well plates were maintained in 20% SVF during 16–18 h and then acidified at different intracellular pH values using the nigericin technique (Lacroix et al., 2004). NHE-1 activity was determined by measuring fast $^{22}Na^{+}$ uptakes conducted after treatments aimed at modifying cholesterol membrane content. ■: Control conditions, ▲: 5 min exposure to 2 mM MBCD, ●: 5 min exposure to 40 μM cholesterol following 20 min exposure to MBCD. ×: direct addition of 40 μM cholesterol. Plots represent V/V_{max} values as a function of intracellular H^{+} concentration. The error bars correspond to SEM. Note the increase in NHE-1 cooperative response upon cholesterol depletion and its decrease upon cholesterol addition. B: Modulation of NHE-1 allosteric constant (L_0) by cholesterol. Allosteric constants were calculated from the experimental data presented in part A using the Monod–Wyman–Changeux equation for a dimeric NHE-1. The number of independent experiments is provided in the figure. The errors on the fits are given as error bars. The values presented here correspond to goodness of the fit factors (rsq) higher than 0.9. Note that an increase in the value of L_0 corresponds to an allosteric inhibition of the transporter.

see, Putney et al., 2002), it is only recently that the allosteric characteristics of this transporter has been described. We indeed fitted NHE-1 activity curves according to the Monod–Wyman–Changeux model (Lacroix et al., 2004), thus considerably simplifying the study of kinetic parameters of this transporter. Besides, recent works have also focused on the possible role of NHE-1 as a signaling complex, due to its function of anchoring for cytoskeleton and scaffolding for signaling proteins (for review, see, Baumgartner et al., 2004); however a lot remains to be evaluated regarding these aspects. Similarly, only a few studies have focused on the role of membrane characteristics in the control of NHE-1 activity (Fuster et al., 2004; Cingolani et al., 2005; Alexander and Grinstein, 2006).

In order to gain further insight into the role of membrane in controlling the allosteric activity of NHE-1, the present study was performed to evaluate the role of cholesterol- and caveolin-rich membrane microdomains. We demonstrate for the first time that NHE-1, which is preferentially localized in these microdomains, sees its cooperative regulation by intracellular protons strongly modulated by this feature. Indeed, exposure to cholesterol-depleting agents, which induces a perturbation of membrane microdomains, elicits an activation of NHE-1. Thus, cholesterol content possibly modulates membrane NHE-1 localization in or out of cholesterol-rich domains, and consequently its activity.

Although a role for cholesterol in modulating NHE-1 activity has been previously suggested (for review, see, Bastiaanse et al., 1997), nothing was known about its effect on the kinetics of this transporter. By fitting with the Monod–Wyman–Changeux equation, we have demonstrated for the first time that the L_0 value was reduced upon MBCD or CholOx treatments and enhanced after cholesterol repletion, with no changes in the microscopic affinity constants or in V_{max} in all cases. As seen from the comparisons of Figures 1B and 5B, this effect is observed either in the absence or in the presence of 20% FCS stimulation. Because serum treatment reduces the L_0 value, the effects of cholesterol depletion and repletion, although largely detectable, are comparatively less important in these conditions than in the absence of serum (see the control and MBCD conditions). To further investigate this point, we therefore decided to use two mutants of NHE-1. Regarding the michaelian R327E NHE-1 mutant, characterized by its loss of cooperative activation capacity by H^{+}, a decrease in membrane cholesterol level upon exposure to MBCD restored its cooperative behavior, with the same affinity constant as for the wild type counterpart. Therefore these results point to a cholesterol-dependent NHE-1 regulation through an effect on its allosteric balance characterized by L_0 parameter. Furthermore, when we used the constitutively activated mutant CTER+, which was nearly completely insensitive to growth factors, we observed that cholesterol was still capable of modulating the activity of this mutant. Noticeably, this pointed to independent molecular pathways underlying regulations of NHE-1 by mitogens and cholesterol membrane content.

In this context, one can propose that cholesterol in the proximal environment of the transporter might increase membrane packing, thus exerting a physical constraint on NHE-1 transmembrane region that would displace the allosteric balance to the low affinity form. Perturbations of this nested situation by cholesterol removal (for MBCD) or by cholesterol oxidation (CholOx) would remove this constraint and promote ionic exchange by allowing the allosteric balance to shift toward the high affinity conformation. Such a model is in accordance with the fact that the allosteric balance of NHE-1 is modified, without affecting the microscopic affinities of the proton transport site. It is worth noting here that different transmembrane proteins such as rhodopsin or cholecystokinin receptors have been demonstrated as exhibiting a change in conformation related to an increase in activity upon cholesterol depletion (Albert and Boesze-Battaglia, 2005; Harikumar et al.,

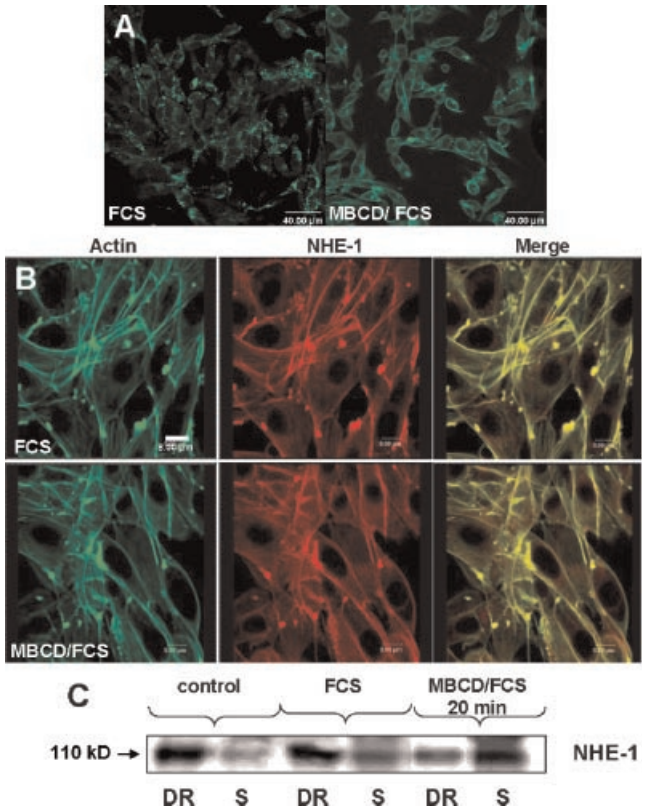

Fig. 6. NHE-1 activation by MBCD or CholOx in presence of serum is also associated with its relocation outside membrane microdomains. PS120-NHE-1 cells were treated or not with 2 mM MBCD, for 20 min (A–C), in presence of 20% FCS. A: After fixation and permeabilization, immunostaining of cells was performed with Alexa 488 conjugated-cholera toxin subunit B (to visualize GM1 ganglioside; green), followed by an incubation of an anti-Cholera toxin subunit B antibody for crosslinking. Cells were viewed by confocal fluorescence microscopy. The experiments were repeated at least three times, with similar results. B: After fixation and permeabilization, immunostaining of cells was performed with a rabbit polyclonal anti-NHE-1 antibody, fluorescein phalloidin to visualize F-actin (green), and with an anti-rabbit antibody coupled to TRITC (red). Cells were viewed by confocal fluorescence microscopy (magnification 400×). Co-localizations are seen in yellow. The experiments were repeated at least three times, with similar results. C: Western blot analysis of NHE-1 distribution on pooled detergent resistant (DR; 1–7: 5 μg) and soluble (S; 8–11: 100 μg) fractions. Data were representative of at least three independent experiments. [Color figure can be viewed in the online issue, which is available at www.interscience.wiley.com.]

2005). However, depleting membrane cholesterol is also known to result in alterations of membrane microstructure, that is, of membrane cholesterol-enriched microdomains, especially those containing caveolin (Zidovetzki and Levitan, 2007). Examination of NHE-1 distribution in membrane microdomains demonstrated that, even upon a very short exposure to MBCD (5 min, Fig. 4C), the protein was relocated outside cholesterol-and caveolin-rich microdomains, such a change being prevented upon cholesterol replenishment. Activation by relocalization outside membrane microdomains has also been described for other transporters or channels, for example, for glucose transporter (GLUT1) (Barnes et al., 2004) and potassium channel BK (Lam et al., 2004). In contrast, other microdomain-dependent transporters and channels appear to be activated by their entry into microdomains, such as Ca^{2+} channel CD20 (Janas et al., 2005), P-glycoprotein PgP (Troost et al., 2004), sodium-glucose co-transporter SGLT1 (Runembert et al., 2002) or serotonin transporter (Magnani et al., 2004). Thus, NHE-1 would belong to the group of membrane proteins whose positive regulation is correlated to a relocalization of the protein outside cholesterol- and caveolin-rich membrane microdomains. It is worth noting here that treatment of PS120-NHE-1 cells with exogenous sphingomyelinase, which leads, in contrast to MBCD, to clustering of microdomains (Probodh and Johnston, 2007), was found to reduce NHE-1 activation by H^+ (Supplementary Fig. 2). Regarding NHE-3, unlike NHE-1, a decrease in activity upon MBCD exposure has been previously reported in OK cells (Murtazina et al., 2006); such an effect appeared to stem notably from a decrease of the V_{max} of the exchange, which was clearly not the case when considering NHE-1 (see Fig. 1D). Despite this decrease in V_{max} but similar to what was observed for NHE-1 (see Fig. 2), no change in the surface amount of NHE-3 was detected upon MBCD treatment. In our case, one might hypothesize that the redistribution of the exchanger outside cholesterol- and caveolin-rich microdomains would favor the transporter to be closer to one of its activators or far from an inhibitor. For example, such a relocalization might help calmodulin to bind NHE-1, thereby alleviating the inhibiting action of the calmodulin binding site of the exchanger (Wakabayashi et al., 1997). This hypothesis is currently under investigation.

Other membrane parameters may explain NHE-1 activation upon cholesterol depletion such as membrane fluidity, a parameter well known to be modified by cholesterol. One might then propose that NHE-1 allosteric transition to the high affinity form may be enhanced by an increase in the fluidity of its membrane microenvironnement (i.e., in lipid microdomains with a reduced content in cholesterol or outside cholesterol-rich microdomains). However, an increase in membrane fluidity has previously been shown to decrease NHE-1 V_{max} of transport for Na^+ without any change in K_{Na} (Bookstein et al., 1997). By contrast we found no detectable change in V_{max} in our experiments. Another important aspect that would deserve further investigation is related to membrane tension and curvature. Indeed, we have recently observed, similar to Fuster et al. (2004), that membrane deformation by cup formers (chlorpromazine) and crenators (arachidonate) induced an allosteric activation and inhibition of NHE-1, respectively (Lacroix et al., unpublished work). However, no study has yet determined whether membrane deformation involves alterations in caveolae composition or, vice versa, whether changes in lipid microdomains affect membrane curvature. In this context, since NHE-1 is preferentially located into caveolae, we could hypothesize that caveolins could act as mechanical sensors, converting membrane constraints into intracellular signals, as it has been previously suggested in endothelial cells (Sedding et al., 2005).

Another important aspect of our work was to test whether the membrane control of NHE-1 evidenced here was occurring *via* a similar pathway as for mitogenic regulation of the transporter, that is, through C-terminal domain phosphorylations (Bianchini et al., 1997). We have therefore examined activation by both MBCD and growth factors supplied by serum. Our experiments with co-treatments with MBCD and FCS clearly suggested that NHE-1 was activated according to different pathways. First, we observed a cumulative effect of both stimuli on NHE-1 activity. Second, FCS did not affect NHE-1 localization while activating it. Third, MBCD was capable to over-activate the R327E mutant form in presence of FCS and, overall, to activate the CTER+ mutant, which corresponds to a constitutively active form of NHE-1 (i.e., nearly completely insensitive to FCS). In total, all these arguments strongly support a NHE-1 regulation pathway up to now not described, dependent on membrane cholesterol composition and microstructure, and different from the

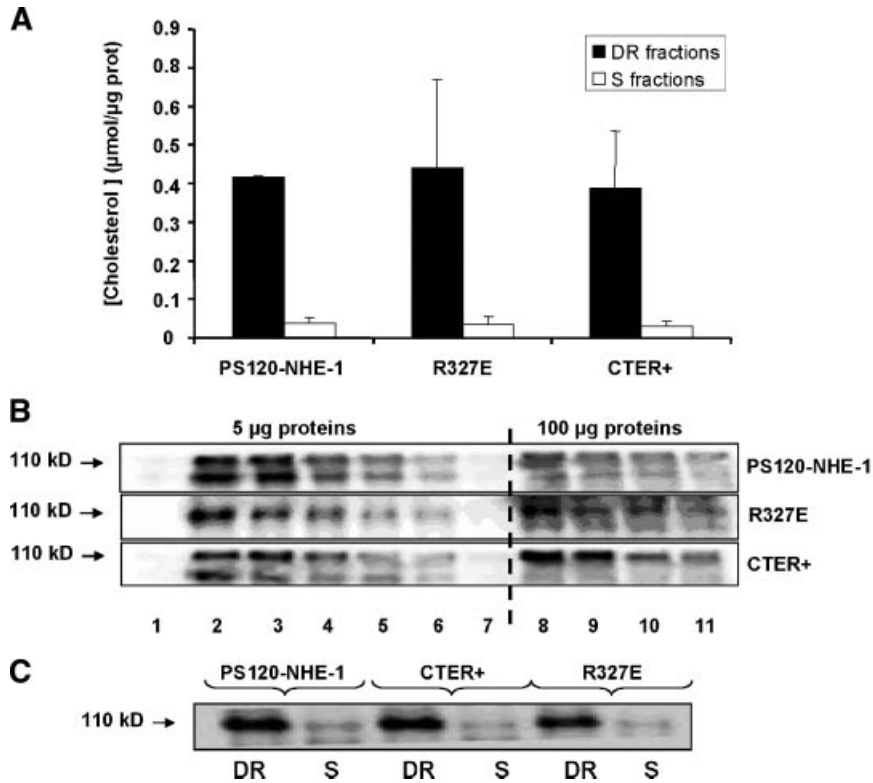

Fig. 7. Low affinity NHE-1 mutant (R327E) and constitutively activated NHE-1 mutant (CTER+) cells exhibit the same levels of cholesterol and NHE-1 into lipid microdomains compared to PS120-NHE-1 cells. Membrane microdomains were isolated as described in Materials and Methods Section, from untreated PS120-NHE-1, R327E mutant and CTER+ mutant cells. A: Estimation of cholesterol content in DR and S fractions in PS120-NHE-1, R327E mutant and CTER+ mutant cells. N = 3 independent experiments. B: Western blot analysis of NHE-1 distribution during cholesterol-rich domain fractionation in PS120-NHE-1, R327E mutant and CTER+ mutant cells. Five and 100 µg were loaded for 1–7 and 8–11 fractions, respectively. C: Western blot analysis of NHE-1 distribution on pooled detergent resistant (DR; 1–7: 5 µg) and soluble (S; 8–11: 100 µg) fractions. Data were representative of at least three independent experiments.

mitogenic pathway. However, it was not excluded that MBCD, by activating signaling cascades, may consequently lead to NHE-1 activation, notably via MAP kinases (Furuchi and Anderson, 1998; Wang et al., 2005). Analysis of phosphorylation profiles of ERK, p38 kinase and JNK were thus performed and revealed an activation of ERK following MBCD exposure under our experimental conditions. Measurements of NHE-1 activity in the presence of an inhibitor of MKK1, which prevents ERK phosphorylation, showed that MBCD-induced NHE-1 activation relied neither upon ERK nor upon other MAPK activation. This might thus point to the prominent role for membrane environment in the NHE-1-regulation. These conclusions have to be related to those obtained from studies on the effects of osmotic pressure. Indeed, Gillis et al. (2001), as well as our team (Lacroix et al., unpublished work) have also predicted a NHE-1 regulation pathway independently of canonical signaling pathways. Considering all these data, the present work thus reinforces the idea that NHE-1, like channels, may be mechanosensitive and can oscillate between an inactive and an active form.

On a pathophysiological point of view, repercussions of the cholesterol and caveolae-dependent NHE-1 regulation may be various, since NHE-1 is an ubiquitous transporter implicated in multiple cellular functions (pH_i and cell volume regulation, $[Na^+]_i$ homeostasis, signaling, mobility, etc.). Indeed, numerous diseases are known to be related to alterations in lipid synthesis and oxidation: atherosclerosis, obesity, diabetes, lysosomal storage diseases (Niemann-Pick disease type C), Alzheimer disease,. . . (for review, see, Maxfield and Tabas, 2005). Knowing that NHE-1 activity has already been described to be altered in some of these pathologies (Lagadic-Gossmann et al., 1988; LaPointe and Batlle, 1994; Urcelay et al., 2001; Bourikas et al., 2003; Jung et al., 2004), one might then expect a link, still to be established, between alterations of lipid synthesis and oxidation and those of NHE-1 activity. Moreover, during various cell dysfunctions, notably in heart (ischemia/reperfusion sequence, anoxia, or metabolic inhibition), a decrease of cholesterol content has been detected (Bastiaanse et al., 1997); in these cases, NHE-1 is also known to be activated and to be responsible for heart injury (Pedersen et al., 2006). In this context, cholesterol may be a new factor to consider when studying the role of NHE-1 activity in the development of disease-related alterations.

In conclusion, this study demonstrates a new NHE-1 regulation pathway. This pathway is important and original for at least three reasons: first, it does not involve a direct modification of the protein by canonical signaling pathways, but secondly, it involves instead the transporter membrane environment, that is, cholesterol- and caveolin-enriched microdomains. Third, this work presents the first demonstration of a negative regulation mechanism of NHE-1 sensitivity to intracellular protons due to membrane environment. This is conceptually important, because such a constitutive negative constraint is required to make NHE-1 activable by other stimuli. Finally, when considering pathological situations and ageing, our results may have major impact

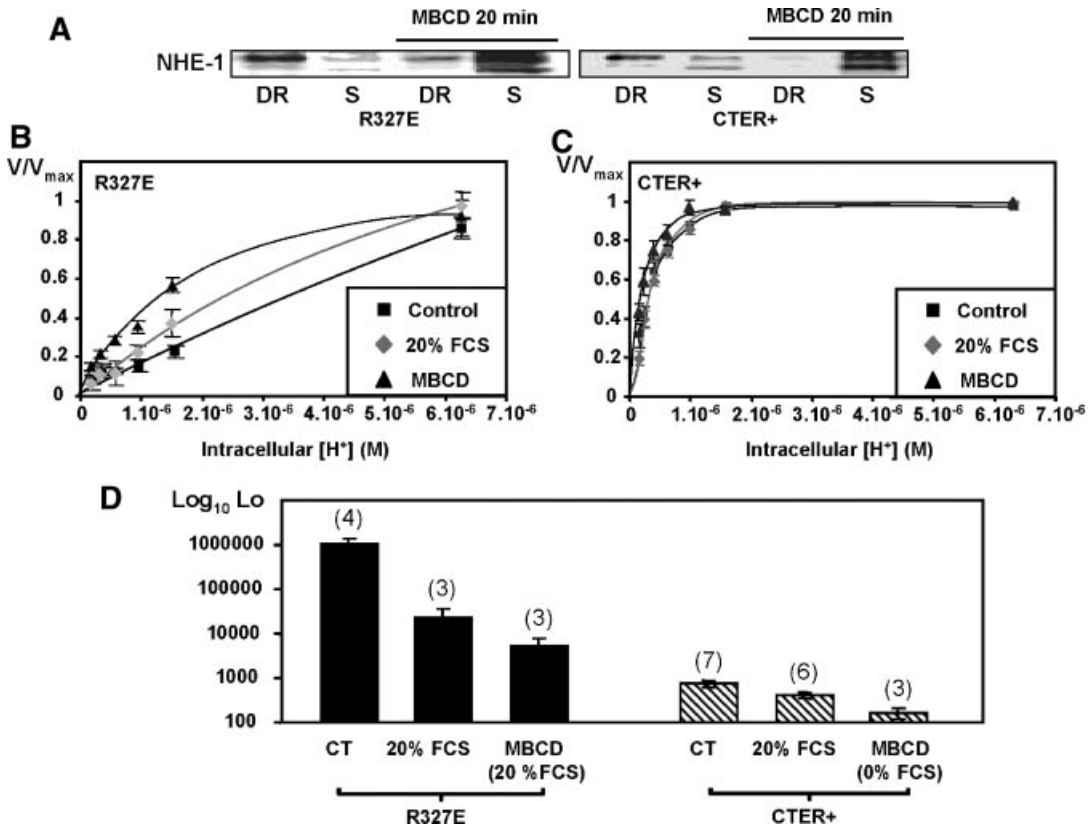

Fig. 8. Low affinity NHE-1 mutant (R327E) and constitutively activated NHE-1 mutant (CTER+) cells are still sensitive to cholesterol depletion. The R327E mutant is a constitutively allosterically inactivated NHE-1 mutant, whilst the CTER+ mutant displays the opposite phenotype. A: Membrane microdomains were isolated as described in Materials and Methods Section, from R327E and CTER+ mutants, either untreated or treated with 2 mM MBCD for 20 min. Western blot analysis of NHE-1 distribution on pooled detergent resistant (DR; 1–7: 5 μg) and soluble (S; 8–11: 100 μg) fractions. Data were representative of at least three independent experiments. B,C: Dose responses of the R327E and CTER+ mutants respectively for intracellular protons, in control conditions (squares), following 20% FCS stimulation (diamonds) or following MBCD treatment (triangles). D: Comparison of the L_0 values for two mutants of NHE-1 allosteric regulation. Initial rates of $^{22}Na^+$ fluxes at different intracellular pH values were measured for the two mutants under the conditions given in the figure. L_0 values were calculated using the Monod–Wyman–Changeux equation for a dimeric NHE-1 (Lacroix et al., 2004). For scale reasons, the Logarithms of L_0 were used to construct the histogram instead of L_0 values themselves. The number of independent experiments is provided in the figure. The errors on the fits are given as error bars. The values presented here correspond to goodness of the fit factors (rsq) higher than 0.9. Note that an increase in the value of L_0 corresponds to an allosteric inhibition of the transporter.

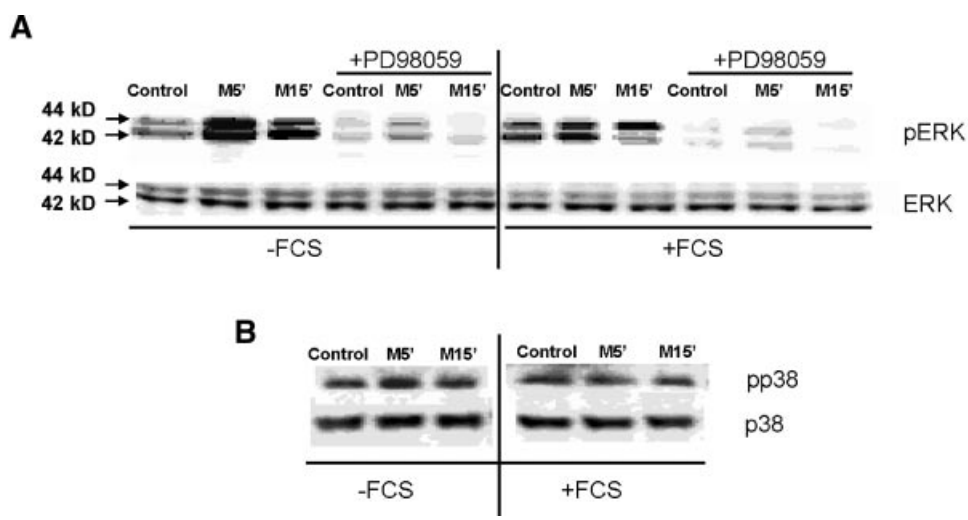

Fig. 9. The MBCD elicited activation of ERK Western blot analysis of ERK (A) and p38 (B) phosphorylation and of total ERK (A) and p38 (B) content following MBCD (2 mM) exposure for 5 and 15 min, in presence or not of 20% FCS in PS120-NHE-1 (total lysates). In (A), the effects of inhibiting the ERK pathway by the chemical compound PD98059 (20 μM) are also presented. Thirty microgram of proteins were loaded. M: MBCD. Data were representative of at least three independent experiments.

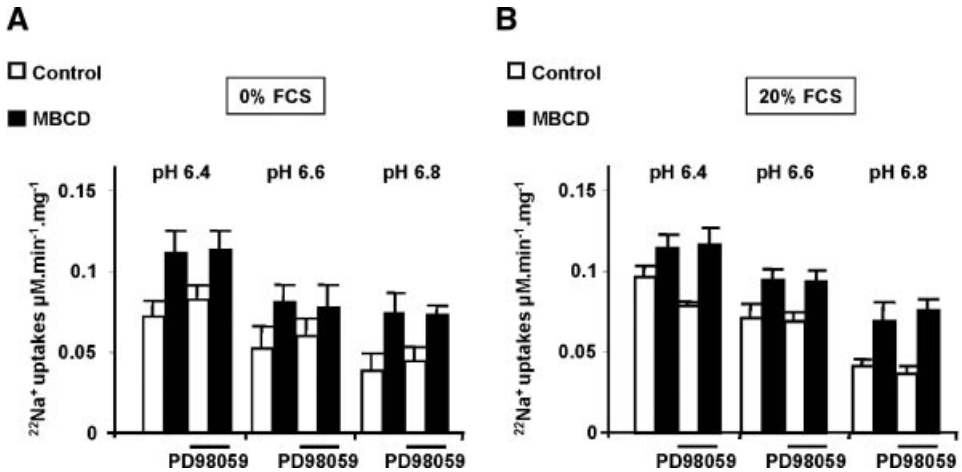

Fig. 10. ERK activation by MBCD is not responsible for NHE-1 activation (A,B) NHE-1 activity was measured at various acidic pH, following MBCD treatment (2 mM, 5 min), in presence or not of PD98059, and 0% (A) or 20% FCS (B).

because they establish for the first time a clear link between membrane lipid content, noticeably cholesterol, and intracellular pH regulation.

Acknowledgments

We wish to thank the microscopy platform and Dr Dutertre (IFR 140, CNRS, Rennes) for helpful advice on immunolocalization captures and analysis. We also wish to thank Roselyne Primault (Department of Microscopy, University of Rennes 1) for confocal analysis. We are very grateful to Gwénaelle Le Moigne for helpful technical advice about lipid microdomain isolation.

Literature Cited

Albert AD, Boesze-Battaglia K. 2005. The role of cholesterol in rod outer segment membranes. Prog Lipid Res 44:99–124.
Alexander RT, Grinstein S. 2006. Na+/H+ exchangers and the regulation of volume. Acta Physiol (Oxf) 187:159–167.
Avkiran M, Haworth RS. 2003. Regulatory effects of G protein-coupled receptors on cardiac sarcolemmal Na+/H+ exchanger activity: Signalling and significance. Cardiovasc Res 57:942–952.
Barclay M, Cogin GE, Escher GC, Kaufman RJ, Kidder ED, Petermann ML. 1955. Human plasma lipoproteins, I. In normal women and in women with advanced carcinoma of the breast. Cancer 8:253–260.
Barnes K, Ingram JC, Bennett MD, Stewart GW, Baldwin SA. 2004. Methyl-beta-cyclodextrin stimulates glucose uptake in Clone 9 cells: A possible role for lipid rafts. Biochem J 378:343–351.
Bastiaanse EM, Hold KM, Van der Laarse A. 1997. The effect of membrane cholesterol content on ion transport processes in plasma membranes. Cardiovasc Res 33:272–283.
Battisti WP, Palmisano J, Keane WE. 2003. Dyslipidemia in patients with type 2 diabetes. Relationships between lipids, kidney disease and cardiovascular disease. Clin Chem Lab Med 41:1174–1181.
Baumgartner M, Patel H, Barber DL. 2004. Na(+)/H(+) exchanger NHE-1 as plasma membrane scaffold in the assembly of signaling complexes. Am J Physiol Cell Physiol 287:C844–C850.
Bertrand B, Wakabayashi S, Ikeda T, Pouyssegur J, Shigekawa M. 1994. The Na+/H+ exchanger isoform 1 (NHE-1) is a novel member of the calmodulin-binding proteins. Identification and characterization of calmodulin-binding sites. J Biol Chem 269:13703–13709.
Bianchini L, L'Allemain G, Pouyssegur J. 1997. The p42/p44 mitogen-activated protein kinase cascade is determinant in mediating activation of the Na+/H+ exchanger (NHE-1 isoform) in response to growth factors. J Biol Chem 272:271–279.
Bookstein C, Musch MW, Dudeja PK, McSwine RL, Xie Y, Brasitus TA, Rao MC, Chang EB. 1997. Inverse relationship between membrane lipid fluidity and activity of Na+/H+ exchangers, NHE-1 and NHE3, in transfected fibroblasts. J Membr Biol 160:183–192.
Bourguignon LY, Singleton PA, Diedrich F, Stern R, Gilad E. 2004. CD44 interaction with Na+-H+ exchanger (NHE-1) creates acidic microenvironments leading to hyaluronidase-2 and cathepsin B activation and breast tumor cell invasion. J Biol Chem 279:26991–27007.
Bourikas D, Kaloyianni M, Bougoulia M, Zolota Z, Koliakos G. 2003. Modulation of the Na(+)-H(+) antiport activity by adrenaline on erythrocytes from normal and obese individuals. Mol Cell Endocrinol 205:141–150.
Bullis BL, Li X, Singh DN, Berthiaume LG, Fliegel L. 2002. Properties of the Na+/H+ exchanger protein. Detergent-resistant aggregation and membrane microdistribution. Eur J Biochem 269:4887–4895.
Cardone RA, Casavola V, Reshkin SJ. 2005. The role of disturbed pH dynamics and the Na+/H+ exchanger in metastasis. Nat Rev Cancer 5:786–795.
Cingolani HE, Perez NG, Aiello EA, de Hurtado MC. 2005. Intracellular signaling following myocardial stretch: An autocrine/paracrine loop. Regul Pept 128:211–220.
Counillon L, Pouyssegur J. 2000. The expanding family of eucaryotic Na(+)/H(+) exchangers. J Biol Chem 275:1–4.
Counillon L, Pouysségur J, Reithmeier RA. 1994. The Na+/H+ exchanger NHE-1 possesses N- and O-linked glycosylation restricted to the first N-terminal extracellular domain. Biochemistry 33:10463–10469.
Denker SP, Huang DC, Orlowski J, Furthmayr H, Barber DL. 2000. Direct binding of the Na–H exchanger NHE-1 to ERM proteins regulates the cortical cytoskeleton and cell shape independently of H(+) translocation. Mol Cell 6:1425–1436.
Dudley DT, Pang L, Decker SJ, Bridges AJ, Saltiel AR. 1995. A synthetic inhibitor of the mitogen-activated protein kinase cascade. Proc Natl Acad Sci USA 92:7686–7689.
Eckert GP, Igbavboa U, Muller WE, Wood WG. 2003. Lipid rafts of purified mouse brain synaptosomes prepared with or without detergent reveal different lipid and protein domains. Brain Res 962:144–150.
Folch J, Lees M, Sloane Stanley GH. 1957. A simple method for the isolation and purification of total lipides from animal tissues. J Biol Chem 226:497–509.
Furuchi T, Anderson RG. 1998. Cholesterol depletion of caveolae causes hyperactivation of extracellular signal-related kinase (ERK). J Biol Chem 273:21099–21104.
Fuster D, Moe OW, Hilgemann DW. 2004. Lipid- and mechanosensitivities of sodium/hydrogen exchangers analyzed by electrical methods. Proc Natl Acad Sci USA 101:10482–10487.
Gadda G, Wels G, Pollegioni L, Zucchelli S, Ambrosius D, Pilone MS, Ghisla S. 1997. Characterization of cholesterol oxidase from *Streptomyces hygroscopicus* and *Brevibacterium sterolicum*. Eur J Biochem 250:369–376.
Garnovskaya MN, Mukhin YV, Vlasova TM, Raymond JR. 2003. Hypertonicity activates Na+/H+ exchange through Janus kinase 2 and calmodulin. J Biol Chem 278:16908–16915.
Gillis D, Shrode LD, Krump E, Howard CM, Rubie EA, Tibbles LA, Woodgett J, Grinstein S. 2001. Osmotic stimulation of the Na+/H+ exchanger NHE-1: Relationship to the activation of three MAPK pathways. J Membr Biol 181:205–214.
Gorria M, Huc L, Sergent O, Rebillard A, Gaboriau F, Dimanche-Boitrel MT, Lagadic-Gossmann D. 2006. Protective effect of monosialoganglioside GM1 against chemically induced apoptosis through targeting of mitochondrial function and iron transport. Biochem Pharmacol 72:1343–1353.
Harikumar KG, Puri V, Singh RD, Hanada K, Pagano RE, Miller LJ. 2005. Differential effects of modification of membrane cholesterol and sphingolipids on the conformation, function, and trafficking of the G protein-coupled cholecystokinin receptor. J Biol Chem 280:2176–2185.
Huc L, Sparfel L, Rissel M, Dimanche-Boitrel MT, Guillouzo A, Fardel O, Lagadic-Gossmann D. 2004. Identification of Na+/H+ exchange as a new target for toxic polycyclic aromatic hydrocarbons. FASEB J 18:344–346.
Huc L, Tekpli X, Holme JA, Rissel M, Solhaug A, Gardyn C, Le Moigne G, Gorria M, Dimanche-Boitrel MT, Lagadic-Gossmann D. 2007. c-Jun NH2-terminal kinase-related Na+/H+ exchanger isoform 1 activation controls hexokinase II expression in benzo(a)pyrene-induced apoptosis. Cancer Res 67:1696–1705.
Janas E, Priest R, Wilde JI, White JH, Malhotra R. 2005. Rituxan (anti-CD20 antibody)-induced translocation of CD20 into lipid rafts is crucial for calcium influx and apoptosis. Clin Exp Immunol 139:439–446.
Jung O, Albus U, Lang HJ, Busch AE, Linz W. 2004. Effects of acute and chronic treatment with the sodium hydrogen exchanger 1 (NHE-1) inhibitor cariporide on myocardial infarct mass in rabbits with hypercholesterolaemia. Basic Clin Pharmacol Toxicol 95:24–30.
Karmazyn M. 1996. The sodium-hydrogen exchange system in the heart: Its role in ischemic and reperfusion injury and therapeutic implications. Can J Cardiol 12:1074–1082.

Karmazyn M. 2001. Role of sodium-hydrogen exchange in cardiac hypertrophy and heart failure: A novel and promising therapeutic target. Basic Res Cardiol 96:325–328.
Khaled AR, Moor AN, Li A, Kim K, Ferris DK, Muegge K, Fisher RJ, Fliegel L, Durum SK. 2001. Trophic factor withdrawal: p38 mitogen-activated protein kinase activates NHE-1, which induces intracellular alkalinization. Mol Cell Biol 21:7545–7557.
Kilsdonk EP, Yancey PG, Stoudt GW, Bangerter FW, Johnson WJ, Phillips MC, Rothblat GH. 1995. Cellular cholesterol efflux mediated by cyclodextrins. J Biol Chem 270:17250–17256.
Lacroix J, Poet M, Maehrel C, Counillon L. 2004. A mechanism for the activation of the Na/H exchanger NHE-1 by cytoplasmic acidification and mitogens. EMBO Rep 5:91–96.
Lagadic-Gossmann D, Chesnais JM, Feuvray D. 1988. Intracellular pH regulation in papillary muscle cells from streptozotocin diabetic rats: An ion-sensitive microelectrode study. Pflugers Arch 412:613–617.
Lagadic-Gossmann D, Huc L, Lecureur V. 2004. Alterations of intracellular pH homeostasis in apoptosis: Origins and roles. Cell Death Differ 11:953–961.
Lagadic-Gossmann D, Huc L, Tekpli X. 2007. Role for Na+/H+ exchanger 1 (NHE1) in the control of apoptotic pathways. In: Pickens CO, editor. Cell apoptotic signaling pathways. Hauppage, NY: Nova Science Publishers. pp 83–114.
Lam RS, Shaw AR, Duszyk M. 2004. Membrane cholesterol content modulates activation of BK channels in colonic epithelia. Biochim Biophys Acta 1667:241–248.
LaPointe MS, Batlle DC. 1994. Na+/H+ exchange and vascular smooth muscle proliferation. Am J Med Sci 307:S9–S16.
Lee AG. 2004. How lipids affect the activities of integral membrane proteins. Biochim Biophys Acta 1666:62–87.
Li X, Galli T, Leu S, Wade JB, Weinman EJ, Leung G, Cheong A, Louvard D, Donowitz M. 2001. Na+-H+ exchanger 3 (NHE3) is present in lipid rafts in the rabbit ileal brush border: A role for rafts in trafficking and rapid stimulation of N HE3. J Physiol 537:537–552.
Magnani F, Tate CG, Wynne S, Williams C, Haase J. 2004. Partitioning of the serotonin transporter into lipid microdomains modulates transport of serotonin. J Biol Chem 279:38770–38778.
Maxfield FR, Tabas I. 2005. Role of cholesterol and lipid organization in disease. Nature 438:612–621.
Mukhin YV, Garnovskaya MN, Ullian ME, Raymond JR. 2004. ERK is regulated by sodium-proton exchanger in rat aortic vascular smooth muscle cells. J Biol Chem 279:1845–1852.
Murtazina R, Kovbasnjuk O, Donowitz M, Li X. 2006. Na+/H+ exchanger NHE3 activity and trafficking are lipid Raft-dependent. J Biol Chem 281:17845–17855.
Okamoto H, Kawaguchi H, Sano H, Kageyama K, Kudo T, Koyama T, Kitabatake A. 1994. Microdynamics of the phospholipid bilayer in cardiomyopathic hamster heart cell membrane. J Mol Cell Cardiol 26:211–218.
Parkin ET, Hussain I, Karran EH, Turner AJ, Hooper NM. 1999. Characterization of detergent-insoluble complexes containing the familial Alzheimer's disease-associated presenilins. J Neurochem 72:1534–1543.
Pedersen SF, O'Donnell ME, Anderson SE, Cala PM. 2006. Physiology and pathophysiology of Na^+/H^+ exchange and Na^+–K^+–2Cl cotransport in the heart, brain, and blood. Am J Physiol Regul Integr Comp Physiol 291:R1–R25.
Poet M, Tauc M, Lingueglia E, Cance P, Poujeol P, Lazdunski M, Counillon L. 2001. Exploration of the pore structure of a peptide-gated Na+ channel. EMBO J 20:5595–5602.
Pouyssegur J, Sardet C, Franchi A, L'Allemain G, Paris S. 1984. A specific mutation abolishing Na+/H+ antiport activity in hamster fibroblasts precludes growth at neutral and acidic pH. Proc Natl Acad Sci USA 81:4833–4837.
Probodh I, Johnston LJ. 2007. Sphingomyelinase generation of ceramide promotes clustering of nanoscale domains in supported bilayer membranes. BBA Biomembranes DOI: 10.1016j.bbamem.2007.09.021.
Putney LK, Denker SP, Barber DL. 2002. The changing face of the Na+/H+ exchanger, NHE-1: Structure, regulation, and cellular actions. Annu Rev Pharmacol Toxicol 42:527–552.
Runembert I, Queffeulou G, Federici P, Vrtovsnik F, Colucci-Guyon E, Babinet C, Briand P, Trugnan G, Friedlander G, Terzi F. 2002. Vimentin affects localization and activity of sodium-glucose cotransporter SGLT1 in membrane rafts. J Cell Sci 115:713–724.
Sardet C, Counillon L, Franchi A, Pouyssegur J. 1990. Growth factors induce phosphorylation of the Na+/H+ antiporter, glycoprotein of 110 kD. Science 247:723–726.
Sedding DG, Hermsen J, Seay U, Eickelberg O, Kummer W, Schwencke C, Strasser RH, Tillmanns H, Braun-Dullaeus RC. 2005. Caveolin-1 facilitates mechanosensitive protein kinase B (Akt) signaling in vitro and in vivo. Circ Res 96:635–642.
Shrode LD, Tapper H, Grinstein S. 1997. Role of intracellular pH in proliferation, transformation, and apoptosis. J Bioenerg Biomembr 29:393–399.
Snabaitis AK, D'Mello R, Dashnyam S, Avkiran M. 2006. A novel role for protein phosphatase 2A in receptor-mediated regulation of the cardiac sarcolemmal Na+/H+ exchanger NHE-1. J Biol Chem 281:20252–20262.
Song KS, Li S, Okamoto T, Quilliam LA, Sargiacomo M, Lisanti MP. 1996. Co-purification and direct interaction of Ras with caveolin, an integral membrane protein of caveolae microdomains. Detergent-free purification of caveolae microdomains. J Biol Chem 271:9690–9697.
Touret N, Poujeol P, Counillon L. 2001. Second-site revertants of a low-sodium-affinity mutant of the Na+/H+ exchanger reveal the participation of TM4 into a highly constrained sodium-binding site. Biochemistry 40:5095–5101.
Troost J, Lindenmaier H, Haefeli WE, Weiss J. 2004. Modulation of cellular cholesterol alters P-glycoprotein activity in multidrug-resistant cells. Mol Pharmacol 66:1332–1339.
Urcelay E, Ibarreta D, Parrilla R, Ayuso MS, Martin-Requero A. 2001. Enhanced proliferation of lymphoblasts from patients with Alzheimer dementia associated with calmodulin-dependent activation of the na+/H+ exchanger. Neurobiol Dis 8:289–298.
Wakabayashi S, Ikeda T, Iwamoto T, Pouysségur J, Shigekawa M. 1997. Calmodulin-binding autoinhibitory domain controls "pH-sensing" in the Na+/H+ exchanger NHE1 through sequence-specific interaction. Biochemistry 36:12854–12861.
Wang PY, Weng J, Anderson RG. 2005. OSBP is a cholesterol-regulated scaffolding protein in control of ERK 1/2 activation. Science 307:1472–1476.
Willoughby D, Masada N, Crossthwaite AJ, Ciruela A, Cooper DM. 2005. Localized Na+/H+ exchanger 1 expression protects Ca2+-regulated adenylyl cyclases from changes in intracellular pH. J Biol Chem 280:30864–30872.
Young M, Funder J. 2003. Mineralocorticoid action and sodium-hydrogen exchange: Studies in experimental cardiac fibrosis. Endocrinology 144:3848–3851.
Zidovetzki R, Levitan I. 2007. Use of cyclodextrins to manipulate plasma membrane cholesterol content: Evidence, misconceptions and control strategies. Biochim Biophys Acta 1768:1311–1324.